JETIR.ORG ISSN: 2349-5162 | ESTD Year : 2014 | Monthly Issue
JOURNAL OF EMERGING TECHNOLOGIES AND INNOVATIVE RESEARCH (JETIR)
An International Scholarly Open Access, Peer-reviewed, Refereed Journal

Numerical analysis of Leak Flow through narrow cracks from high-pressure pipelines

Sandip **Ghosh***, Allen Vivian **Lakra,** Suraj **Gazi,** Suvankar **Debnath,** Santanu **Ghosh,** Abir **Mukherjee**

Department of Mechanical Engineering, JIS College of Engineering, Kalyani, India
Corresponding author ID: sandip.ghosh@jiscollege.ac.in

Abstract. *The occurrence of cracks in high-pressure duct systems is common and has been proven to be hazardous for various power and process plants. Safety issues are driven by piping design methodology and loss-of-coolant accident scenarios, especially in nuclear power stations. The present work analyses the leak flow through narrow circumferential cracks on stainless steel pipes of predefined geometry at varying high-pressure water conditions and different areas of crack openings using computational simulation methods. The results of this analysis showcase the behaviour of leak flow properties flowing through the crack perpendicular to the main flow for a set of boundary conditions. The results indicate that at normal temperature, the leak flow pattern is primarily driven by the stagnation pressure for single-phase leaks. Generated data for high-pressure pipelines is applicable for various industrial scenarios, crucial for crack detection and safety measures before any severe accident occurs.*

1. Introduction

The pipeline in a power plant is a significant part that deals with the transportation of fluids. High-pressure system design requires a mandatory safety analysis through the methodology of Leak Before Break (LBB). This is a cost-efficient and sustainable methodology for piping design where the formation and growth of cracks due to corrosion, erosion and other defects are scrutinised before the entire system experiences a disruption. The primary system pipelines in nuclear reactors carry radioactive substances, and safety is a prime concern. Therefore, measurements of leak, along with detection of leak, are a part and parcel of LBB analysis, which also offers valuable information on probable crack morphology [1]. These phenomena are quite usual in various oil or gas transporting pipelines, causing pipeline leakage. If not monitored carefully, leakages can have massive impacts on human and marine life [2]. The application of the Finite Element Method in studying fracture mechanics has been well documented in various literature discussing pipeline integrity and the interactions caused by corrosion defects [3,4]. Advanced numerical techniques have been employed to accurately determine the extent of crack growth that occurs as a result of stress corrosion cracking [5]. Additionally, these techniques have also been used to analyse the through-wall cracks that may occur under high-temperature and high-pressure pipe flow [6]. Some numerical techniques have been used to determine leak flow through a crack and the corresponding through-wall crack opening under high-pressure [7]. By utilising these methods, engineers can gain critical insights into the behaviour of materials subjected to extreme environments and develop effective strategies to mitigate the risk of catastrophic failures for sustainable development.

In the applications of high-pressure pipelines used in several power plants and chemical industries, various materials are used based on their unique properties. Carbon steel can withstand high temperatures and but it faces corrosion when exposed to moisture, chemicals and acids [8]. To mitigate this, protective coatings are applied to the surface of the pipelines. Stainless steel, on the other hand, is regarded as one of the ideal materials used in various pipelines. It is highly resistant to corrosion, even in acidic and high-moisture environments. Despite the associated cost, its durability and corrosion-resistant properties make it a preferred choice in various industries, inclusive of Nuclear Power Plants [10]. Pipelines often have a type of damage called a dent crack, which looks like a semi-ellipse. Several crack detection techniques using sensors have been reported in the literature [11]. Several studies have focussed on the determination of critical leak flow evaluations through predefined cracks or slits through theoretical and experimental investigations [12-14]. CFD simulations have emerged as a popular alternative regarding the prediction of leakage mass flux under a variety of boundary conditions [15]. However, there is a lot of scope to simulate various analytical models to evaluate the effect of stagnation pressure and crack morphology on pipe leaks, causing severe accidents in key power stations.

This paper aims to analyse the behaviour of a high-pressure pipeline with a predefined circumferential crack of rectangular and circular profile under various pressure conditions. Mass flow rate and leakage flow patterns have been studied for various boundary conditions through CFD simulation techniques to address a sustainable solution regarding loss-of-coolant accidents, especially faced in nuclear power plants.

2. Physical Problem and Computational Setup

The current CFD analysis has been conducted for a computational domain of water flowing through a circular pipe made of steel. A circumferential crack has been generated through 3D modelling near the middle of the test section. The study has been done by designing leak locations of various circular and rectangular dimensions. This physical problem for CFD analysis represents the actual life scenario of crack formation in the high-pressure pipelines of a duct system of a nuclear power plant.

2.1. Geometry and Mesh

The dimensions of the pipe whose flow domain is taken into account are 500 mm (length) x 100 mm (diameter) having 5 mm thickness. Three circular-shaped minute cracks of diameter 1 mm, 1.5 mm, and 2 mm and three rectangular-shaped narrow cracks of length 1 mm, 2 mm, 3 mm, and breadth 0.5 mm each have been taken into consideration for the analysis. The geometry is designed using the ANSYS Design Modeller tool. The geometry of the flow domain of the circular pipe is shown in Fig. 1 (a). Similarly, Fig. 1 (b) & 1 (c) show a zoomed picture of the small circular crack and the narrow rectangular crack, respectively. The thickness of the pipe is taken into consideration while designing the crack openings. The mesh of the geometry is generated as shown in Fig. 2. The various sections of the geometry are named before generating the mesh, namely, inlet, outlet, pipe wall, crack outlet, and crack wall. In the generated mesh, the average orthogonal quality of 0.99 and average element quality of 0.86 were maintained.

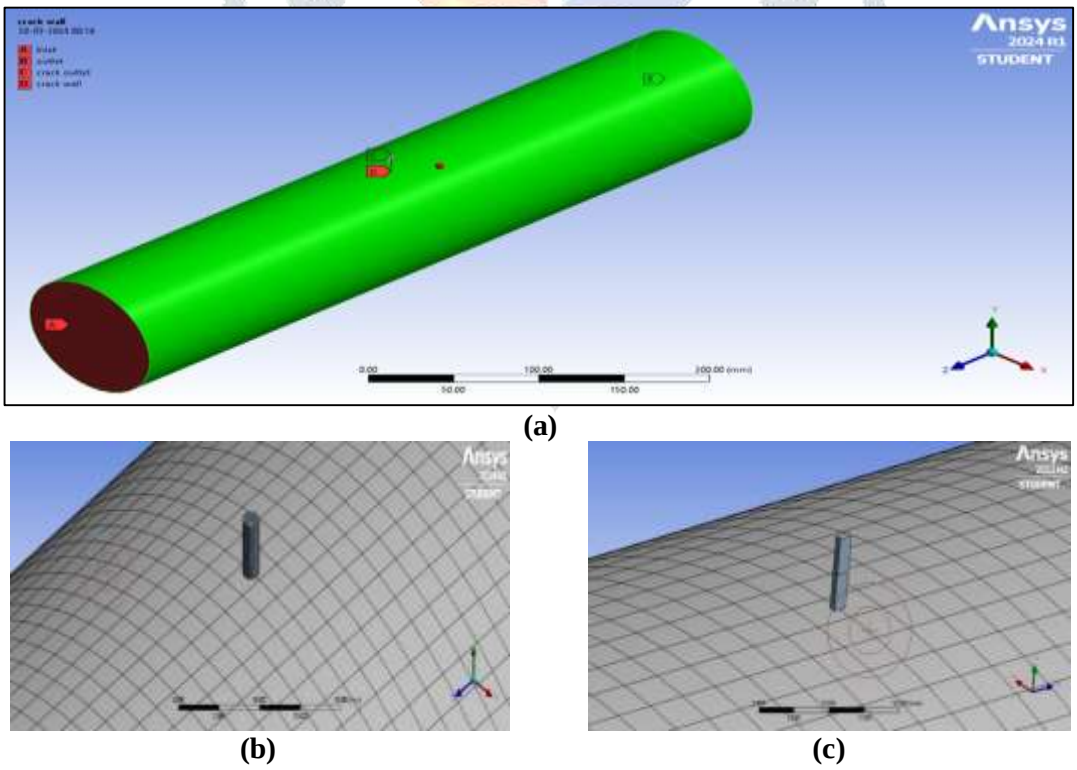

(a)

(b) **(c)**

Figure 1. (a) Computational domain of 500 mm x 100 mm circular pipe with circumferential narrow crack, **(b)** **C**ircular crack geometry, **(c)** Rectangular crack geometry

2.2. Computational setup

The computational fluid dynamics simulation has been performed using the Fluent code on the ANSYS platform. The 3D analysis has been conducted using a double-precision setting. The viscous model used for the setup is k-epsilon. The material selected for the fluid flow domain simulation is water in the liquid state. The boundary conditions given for the simulations are pressure inlet and pressure outlet at the outlet of the flow domain and the crack opening. The pressure set at the inlet ranges from 70 bar to 110 bar, and the pressure set at the outlet ranges from 69 bar to 109 bar, respectively (the pressure difference between the inlet and outlet is kept at 1 bar for all the test cases). The pressure at the crack opening is set at 1 bar, which is the atmospheric pressure under normal conditions. The solution of the continuity and momentum equations was done on the basis of standard convergence criteria.

2.3. Mesh analysis

Simulations were carried out with varying numbers of elements, starting from a coarser mesh and progressing to finer meshes to evaluate grid independence. The data, presented in Figure 2, reveals that as the mesh is refined, the results

exhibit progressively smaller variations. This refinement process was carried out to ensure that the results are reliable while also optimising the computational cost. Based on this analysis, the appropriate mesh was chosen to achieve a balance between accuracy and efficiency for the current study.

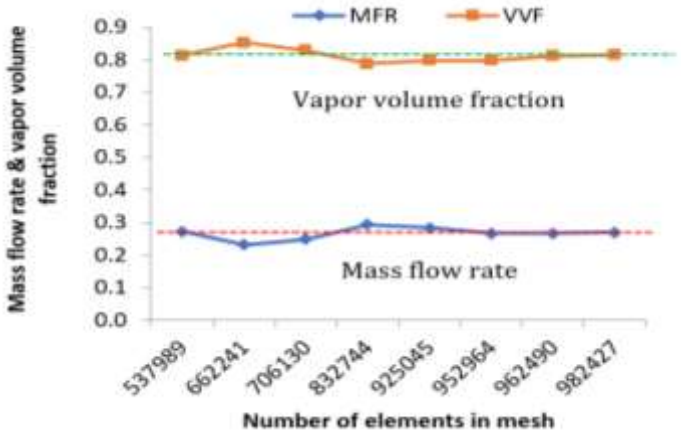

Figure 2: Mass flow rate and vapour volume fraction for different mesh numbers

The computational model set for the present work was validated [Fig.2] against experimental investigations conducted in a similar domain of boundary conditions as reported in the literature [13].

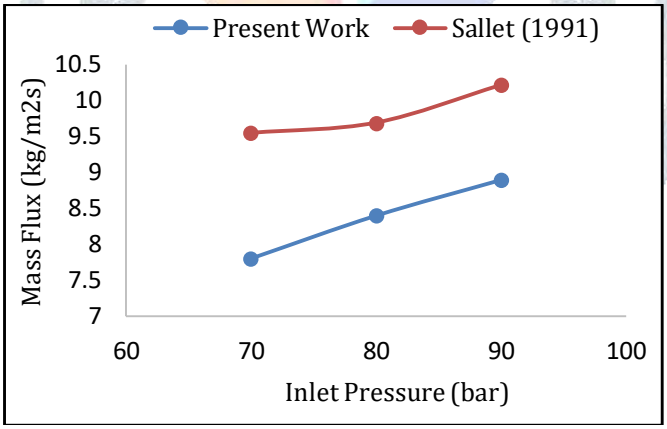

Figure 2. Validation of predicted leak flow behaviour with experimental works [13]

3. Results and Discussion

Tables 1 & 2 show the predicted mass flow rate at the crack location, as calculated by the CFD module for various pressures ranging from 70 bar to 110 bar. To assess the functional relationship between the mass flow rate and crack area at various pressures, the feasible input variations were considered for the analysis. A similar kind of analysis is done for two types of cracks generated at various pressures. The various crack area gives the maximum and minimum mass flow rates.

3.1. Rectangular Crack

Here we have used the steel pipes to analyse the relation between the mass flow rate and the area of the crack. For the rectangular crack under various pressures with various crack areas, the change of mass flux is shown in Table 1. Here, we observed that mass flux increases with the increase in pressure. Throughout the process, the temperature is considered constant. The mass flow rate analysis under various pressures gives the change in mass flux.

Table 1. Predicted mass flux and velocity of leakage through the rectangular crack opening

Sl.	Inlet Pressure (bar)	COA x10^{-6} (m^2)	Mass Flux (kg/m^2s)	Leak flow Velocity (m/s)
1	70	0.5	0.078	86.241
		1	0.081	87.559
		1.5	0.082	88.483
2	80	0.5	0.084	92.358
		1	0.086	93.754
		1.5	0.087	94.682
3	90	0.5	0.089	98.224

		1	0.092	99.673
		1.5	0.093	100.642
4	100	0.5	0.094	103.774
		1	0.097	105.275
		1.5	0.098	106.276
5	110	0.5	0.099	109.193
		1	0.102	110.762
		1.5	0.104	111.829

The variation of the maximum leak flow velocity by the inlet pressure can be depicted from the graph in fig. 3. The maximum leak flow velocity increases with the increase in the pressure at the pipe inlet. Also, the variation of the mass flux with the inlet pressure is shown in the graph in fig. 4. It is seen that the mass flux increases with the increase in the inlet pressure. The pressure and velocity contours found in the simulation result are presented in Figs. 5 and 6.

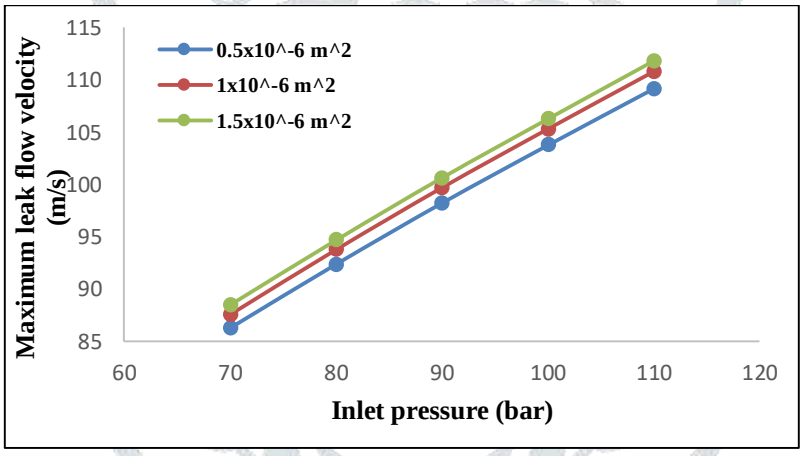

Figure 3. Variation of maximum leak flow velocity with pressure for rectangular cracks

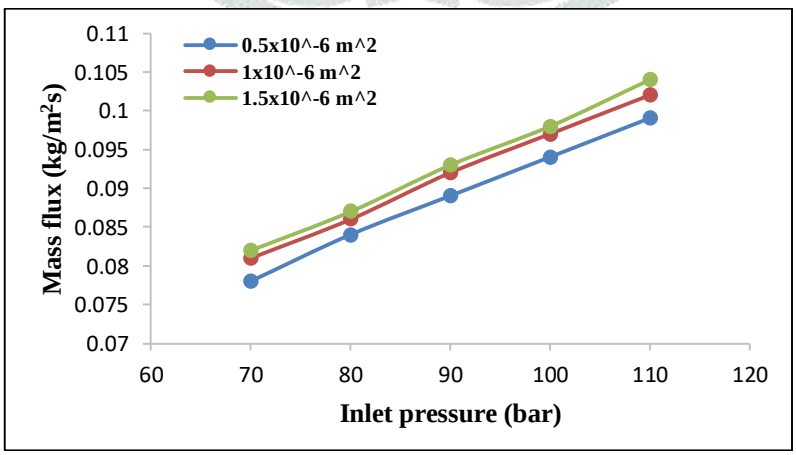

Figure 4. Variation of maximum mass flux with Pressure for rectangular cracks

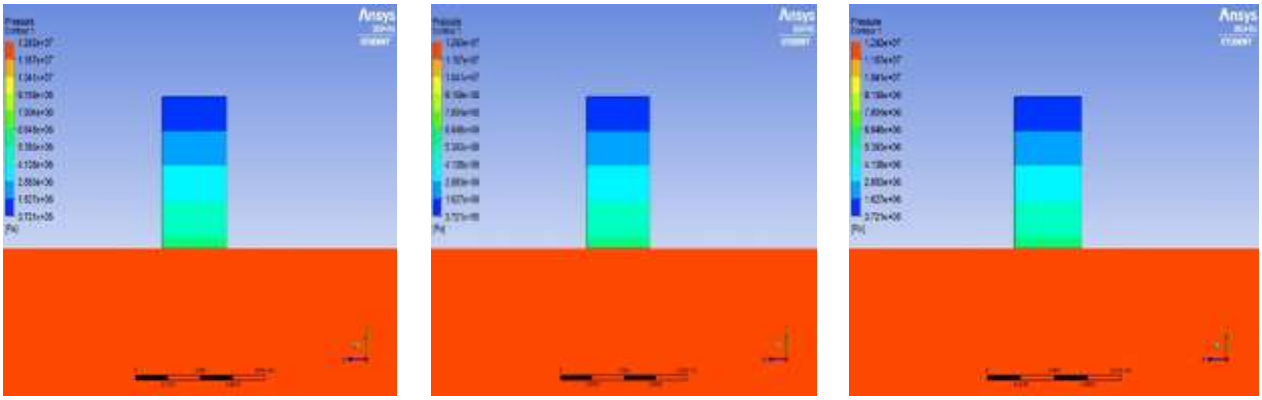

(a) **(b)** **(c)**

Figure 5. Pressure contour of the rectangular crack of 0.5 x 10- 6 m^2 at
(a) 70 bar inlet pressure, **(b)** 80 bar inlet pressure, **(c)** 90 bar inlet pressure

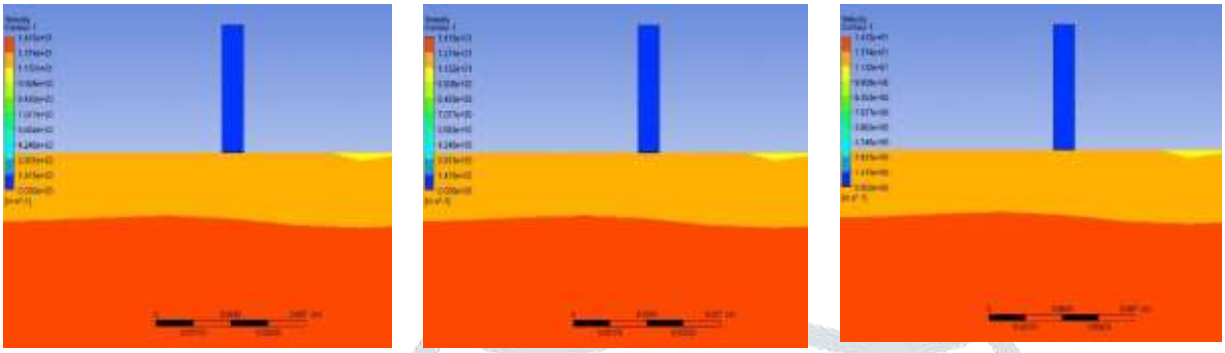

(a) **(b)** **(c)**

Figure 6. Velocity contour of the rectangular crack of area $1.5x10^{-6}$ m^2 at **(a)** 70 bar inlet pressure, **(b)** 80 bar inlet pressure, **(c)** 90 bar inlet pressure

3.2. Circular Crack

The analysis of circular cracks was conducted to determine the relationship between pressure, mass flux, and velocity of the crack. The results of the analysis are presented in Table 2, which shows the changes in mass flux due to variations in pressure and Crack Opening Area (COA). The analysis was conducted under the assumption of constant temperature. The results of the analysis revealed that an increase in pressure led to a corresponding increase in mass flux. The fluid flow rate through the crack was influenced by the pressure gradient and the crack size. Overall, the analysis provides valuable insights into the physics of fluid flow through circular cracks, and it underscores the importance of understanding the underlying mechanisms that govern fluid flow to optimise the design and operation of fluidic systems.

Table 2. Data table of the mass flux and velocity through the circular crack opening at various pressures

Sl.	Inlet Pressure (bar)	COA x 10^{-6}(m^2)	Mass Flux (kg/m^2s)	Leak flow Velocity (m/s)
1	70	7.06	0.027	121.745
		12.56	0.022	98.274
		19.63	0.023	100.441
2	80	7.06	0.027	105.334
		12.56	0.022	104.298
		19.63	0.023	107.552
3	90	7.06	0.023	109.421
		12.56	0.024	110.651
		19.63	0.024	114.457
4	100	7.06	0.024	116.278
		12.56	0.025	115.336
		19.63	0.026	119.548
5	110	7.06	0.026	121.745
		12.56	0.027	121.275
		19.63	0.028	126.354

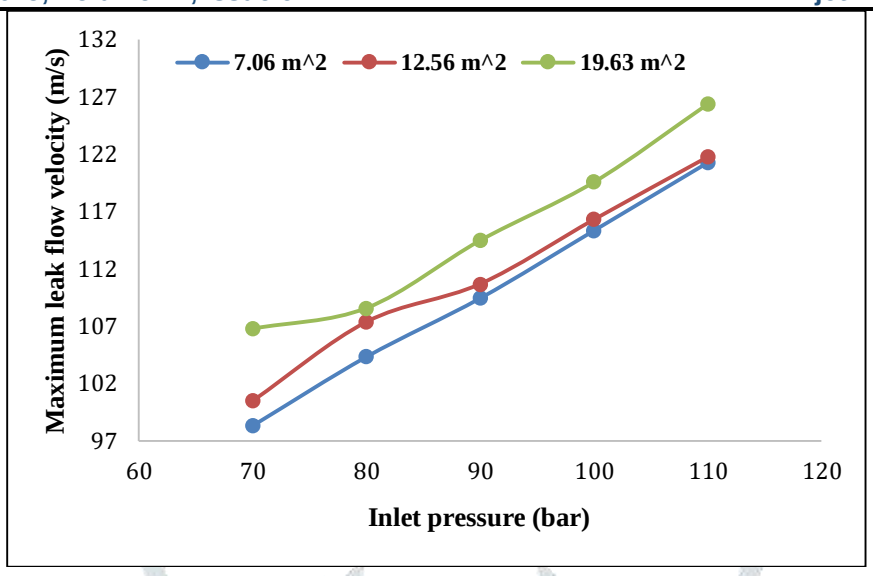

Figure 7. Maximum leak flow velocity vs. Pressure graph for circular cracks

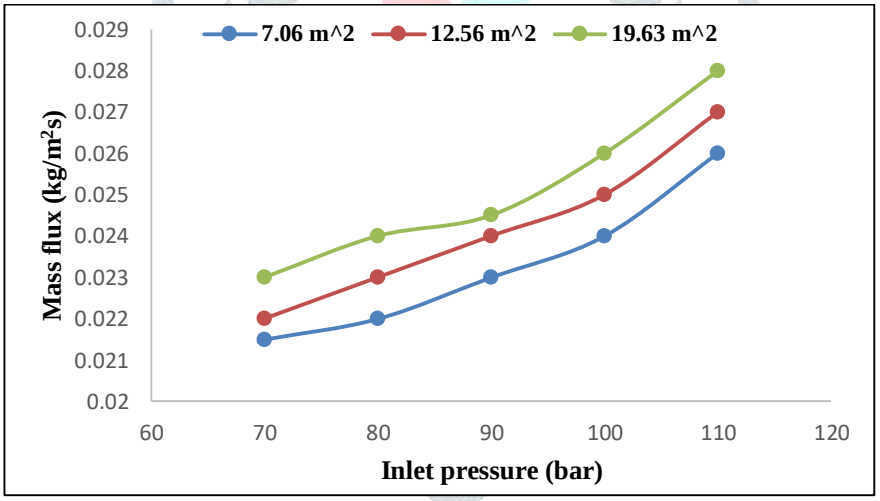

Figure 8. Mass flux vs. Pressure graph

In the case of circular cracks, the variation of the maximum leak flow velocity in accordance with the inlet pressure can be seen in the graph in Figure 7. The maximum leak flow velocity increases with the increase in the pressure at the pipe inlet of the pipe flow domain. Also, the variation of the mass flux with the inlet pressure is shown in the graph in Figure 8. It is seen that the mass flux increases with the increase in the inlet pressure for all the scenarios of leak flow, as reported in some experimental works. The pressure contour presented in fig. 9 shows that the maximum pressure drop inside the narrow slit resulting in critical leakage mass flux and associated velocity contours (fig. 10). Local flow acceleration within the crack and flow stagnation within pipe in nearby crack zone is evident in the contours. The behaviour found in the present work is analogous to several experimental findings [14, 15] as discussed earlier, which enhances the confidence in the model for predicting the high-pressure leak flow behaviour..

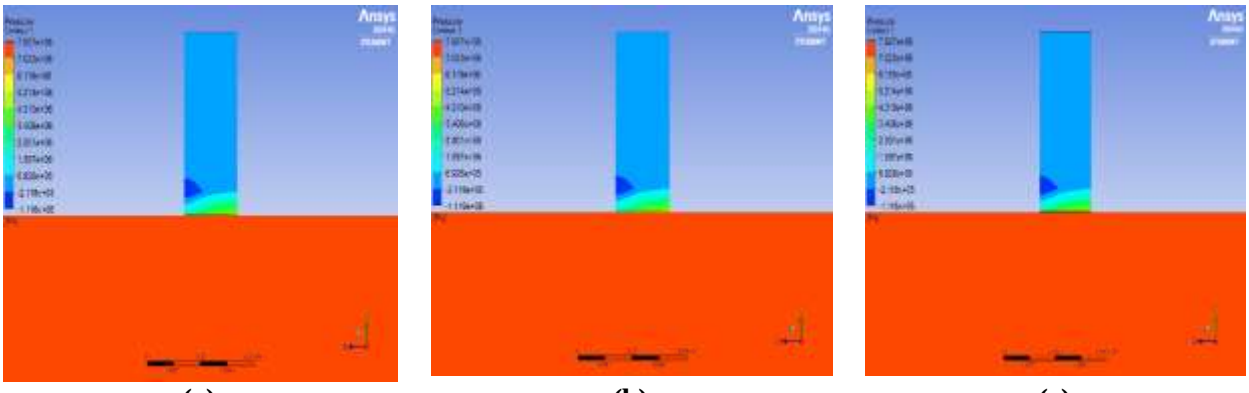

(a) **(b)** **(c)**

Figure 9. Pressure contour image of the circular crack of area 12.56×10^{-6} m^2 at **(a)** 70 bar inlet pressure, **(b)** 80 bar inlet pressure, **(c)** 90 bar inlet pressure

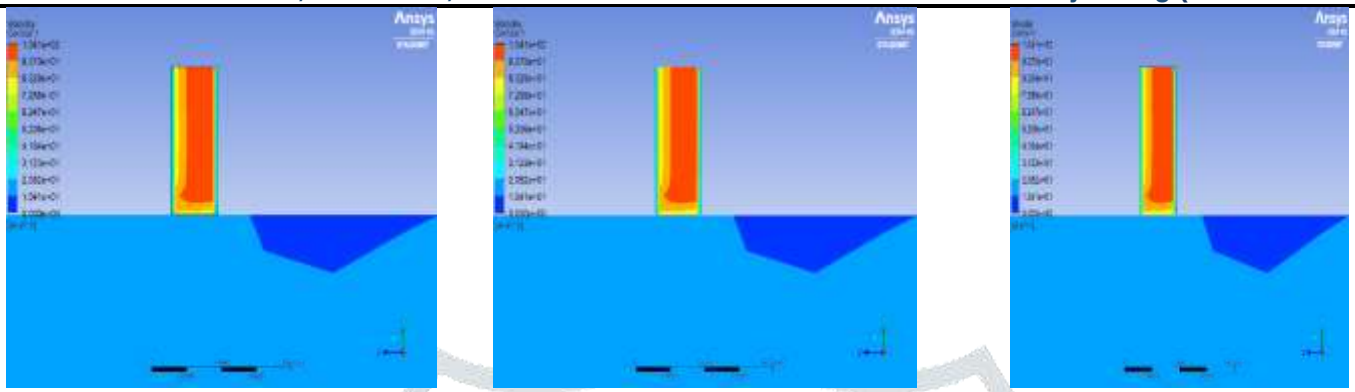

(a) **(b)** **(c)**

Figure 10. Velocity contour image of the circular crack of area 12.56×10^{-6} m^2 at **(a)** 70 bar inlet pressure, **(b)** 80 bar inlet pressure, **(c)** 90 bar inlet pressure

4. Conclusion

Leak flow prediction has been carried out for predefined narrow circular and rectangular circumferential cracks over steel pipes using computational simulations. The result of this analysis demonstrates a range of mass flux during the leakage phenomenon for varying boundary conditions. It is observed that the mass flux through the point of leakage shows an increasing trend with increasing stagnation pressure. Choked flow has been observed while the inlet pressure was varied. These flow variations are critical in determining the severity of the crack and the necessary steps that need to be taken to rectify the situation. Moreover, the increase in pressure correlates with higher mass flux and velocity, potentially exacerbating the crack's size. Therefore, it is essential to monitor the pressure and mass flux to ensure that any potential issues can be identified and addressed promptly to prevent accidental hazards.

5. References

[1] Amos C.N. and Schrock V.E. 1983 Critical Discharge of Initially Subcooled Water through Slits NUREG-CR--3475, USNRC.

[2] Ben-Mansour R. and Khalifa A.E., Computational fluid dynamic simulation of small leaks in water pipelines for direct leak pressure transduction, *Computers & Fluids*, **57**, pp 110-123 **(2012)**.

[3] Chen J.G. and Shi K. Fracture mechanics analysis of cracked structures using weight function and neural network method, Kitakyushu City, pp 10-13, 372 **(2018)**.

[4] Gardner L., The use of stainless steel in structures. Progress, *Structural Engineering and Materials*, **7**, pp 44-55 **(2005)**.

[5] Ghosh S. and Saha S.K., Modelling and Simulation of Subcooled Coolant Loss Through Circumferential Pipe Leakage, *ASME J of Nuclear Rad Sci*., **7(3)**: 034503, **(2021)**. https://doi.org/10.1115/1.4048477

[6] Ghaednia H., Safe burst strength of a pipeline with a dent-crack defect: Effect of crack depth and operating pressure, *Engineering Failure Analysis*, **55,** pp 288–299.

[7] Ghosh S., Mukhopadhyay D., Saha S.K., An experimental analysis of subcooled leakage flow through slits from high pressure high temperature pipelines, *International Journal of Pressure Vessels and Piping*, **88,** pp. 281-289, **(2011)** https://doi.org/10.1016/j.ijpvp.2011.05.008

[8] Huang H.S., Fracture Characteristics Analysis of Pressured Pipeline with Crack Using Boundary Element Method Advances, *Materials Science and Engineering*, pp 1-13 **(2015).**

[9] Kundu A., Ghosh S., Mondal S., Ghosh A. and Roy S., A Comparative Analysis of Sensor-Based Pipe Crack Detection Systems. In: Applications of Networks, Sensors and Autonomous Systems Analytics, *Studies in Autonomic, Data-driven and Industrial Computing*, Springer, Singapore. https://doi.org/10.1007/978-981-16-7305-4_7

[10] Manna S., Kundu A., Dey K., Roy S., Bhuit R. and Ghosh S., CFD simulation of circumferential crack in low-pressure water pipelines, *Materials Today Proceedings*, **80(2)**, pp. 806-812 **(2023)**. https://doi.org/10.1016/j.matpr.2022.11.132

[11] Nam J.Y. and Lee B.Y., The effect of residual stress on the SCC using ANSYS, *Procedia Engineering*, **10,** pp 2609–2614 **(2011)**.

[12] Silva R.C.C. and Loula A.F.D., A Study of Pipe Interacting Corrosion Defects Using the FEM and Neural Networks Advances, *Engineering Software*, **38**, pp 868-875 **(2007)**.

[13] Sallet D.W., Critical mass flow rates through pressure relief valves, College Park, Maryland, USA, Warme und Stoffibertragung **26**, Springer-Verlag, 315-321, **(1991)**.

[14] Sozzi, G. L., and Sutherland, WA 1975. Critical Flow of saturated and subcooled Water at High Pressure, General Electric Company, NEDO-13418, July.

[15] Zhu H., A CFD simulation for oil leakage from a damaged submarine pipeline, *Energy*, **64**, pp 887-899 **(2014)**.